

Received:  
29 May 2018

Revised:  
26 August 2018

Accepted:  
09 September 2018

<https://doi.org/10.1259/bjr.20180479>

Cite this article as:

Jung Y, Gho S-M, Back SN, Ha T, Kang DK, Kim TH. The feasibility of synthetic MRI in breast cancer patients: comparison of  $T_2$  relaxation time with multiecho spin echo  $T_2$  mapping method. *Br J Radiol* 2019; **92**: 20180479.

## FULL PAPER

# The feasibility of synthetic MRI in breast cancer patients: comparison of $T_2$ relaxation time with multiecho spin echo $T_2$ mapping method

<sup>1</sup>YONGSIK JUNG, MD, MS, <sup>2</sup>SUNG-MIN GHO, PhD, <sup>2</sup>SEUNG NAM BACK, MS, <sup>3</sup>TAEYANG HA, MD, <sup>3</sup>DOO KYOUNG KANG, MD, MS and <sup>3</sup>TAE HEE KIM, MD, PhD

<sup>1</sup>Department of Surgery, Ajou University School of Medicine, Suwon, South Korea

<sup>2</sup>MR Clinical Research and Development GE Healthcare, Gangnam, Republic of Korea

<sup>3</sup>Department of Radiology, Ajou University School of Medicine, Suwon, South Korea

Address correspondence to: Dr Tae Hee Kim

E-mail: [medhand@ajou.ac.kr](mailto:medhand@ajou.ac.kr)

**Objective:** To compare the  $T_2$  relaxation times acquired with synthetic MRI to those of multi-echo spin-echo sequences and to evaluate the usefulness of synthetic MRI in the clinical setting.

**Methods:** From January 2017 to May 2017, we included 51 patients with newly diagnosed breast cancer, who underwent additional synthetic MRI and multiecho spin echo (MESE)  $T_2$  mapping sequences. Synthetic MRI technique uses a multiecho and multidelay acquisition method for the simultaneous quantification of physical properties such as  $T_1$  and  $T_2$  relaxation times and proton density image map. A radiologist with 9 years of experience in breast imaging drew region of interests manually along the tumor margins on two consecutive axial sections including the center of tumor mass and in the fat tissue of contralateral breast on both synthetic  $T_2$  map and MESE  $T_2$  map images.

**Results:** The mean  $T_2$  relaxation time of the cancer was 84.75 ms ( $\pm$  15.54) by synthetic MRI and 90.35 ms ( $\pm$  19.22) by MESE  $T_2$  mapping. The mean  $T_2$  relaxation time

of the fat was 129.22 ms ( $\pm$  9.53) and 102.11 ms ( $\pm$  13.9), respectively. Bland-Altman analysis showed mean difference of 8.4 ms for the breast cancer and a larger mean difference of 27.8 ms for the fat tissue. Spearman's correlation test showed that there was significant positive correlation between synthetic MRI and MESE sequences for the cancer ( $r = 0.713$ ,  $p < 0.001$ ) and for the fat ( $r = 0.551$ ,  $p < 0.001$ ). The positive estrogen receptor and low histologic grade were associated with little differences between two methods ( $p = 0.02$  and  $p = 0.043$ , respectively).

**Conclusion:**  $T_2$  relaxation times of breast cancer acquired with synthetic MRI showed positive correlation with those of MESE  $T_2$  mapping. Synthetic MRI could be useful for the evaluation of tissue characteristics by simultaneous acquisition of several quantitative physical properties.

**Advances in knowledge:** Synthetic MRI is useful for the evaluation of  $T_2$  relaxation times of the breast cancers.

## INTRODUCTION

Breast MRI has a high sensitivity for breast cancer and it has been used as a preoperative staging method in patients with newly diagnosed breast cancer,<sup>1-3</sup> as a screening method in high-risk patients,<sup>4-6</sup> and a screening method in patients with personal history of breast cancer.<sup>7-10</sup>

Recently introduced SyMRI is a synthetic MRI technique which can acquire the quantitative physical properties including the longitudinal relaxation rate, transverse relaxation rate and the proton density (PD).<sup>11,12</sup> This technique uses a multiecho and multidelay acquisition method for the simultaneous quantification of these properties.

Several studies have reported the clinical application of synthetic MRI, especially in the brain imaging. Synthetic  $T_1$ - and  $T_2$  weighted images and PD images were acceptable for the diagnosis of multiple sclerosis and for the differentiation of gray/white matter in pediatric patients.<sup>13,14</sup> Krauss et al reported that the synthetic MRI was sufficiently accurate for use in clinical practice showing slight underestimation of  $T_1$  and  $T_2$  relaxation times and slightly overestimation of PD values.<sup>15</sup>

$T_2$  relaxation time is dependent on the chemical component of tissue itself and we can detect the change in tissue component or any pathologic changes using the  $T_2$  relaxation time. There are several studies reporting the clinical

implication of  $T_2$  values in breast cancer patients. The  $T_2$  value was significantly lower in malignant breast lesions than benign lesions.<sup>16</sup> After neoadjuvant chemotherapy,  $T_2$  value was significantly reduced in responders compared to non-responders.<sup>17,18</sup> Intratumoral  $T_2$  high signal intensity has been reported as characteristic finding of triple negative breast cancer<sup>19</sup> and it was associated with the poor response to neoadjuvant chemotherapy.<sup>20</sup> A recent study reported that  $T_2^*$  relaxation time of invasive breast cancer was significantly longer than that of ductal carcinoma *in situ*. Among invasive breast cancers,  $T_2^*$  relaxation time was significantly longer in the cancers having higher histologic grades and high signal intensity on  $T_2$  weighted image.<sup>21</sup>

As far as we know, there has been no research about the application of synthetic MRI to the breast imaging. The purposes of our study were to compare the  $T_2$  relaxation times acquired with synthetic MRI to those of multiecho spin echo (MESE) sequences and to evaluate the usefulness of synthetic MRI in the clinical setting.

## METHODS AND MATERIALS

### Case selection

This retrospective study received Institutional Review Board approval and the requirement for informed consent was waived. From January 2017 to May 2017, 196 patients underwent pre-operative breast MRI for the newly diagnosed breast cancer. The inclusion criteria were MR images of breast cancer patients who were diagnosed as invasive ductal carcinoma, not otherwise specified and who were examined using 3 T MRI with routine protocol sequences, additional synthetic sequences and two-dimensional (2D) fast spin echo MESE sequences for  $T_2$  mapping. We excluded 82 patients who were not scanned on 3 T MRI or not scanned with additional synthetic sequences, 24 patients who were diagnosed as other histologic types of breast cancer, 18 patients who had undergone surgical excision or vacuum-assisted breast biopsy before the breast MRI and 21 patients who

had small cancers which were not visualized on both synthetic MR images and MESE  $T_2$  mapping images. Finally, a total of 51 patients were included and evaluated in this retrospective study. Mean age of 51 patients was 52.11 years old ( $52.11 \pm 9.78$  years old).

### MRI acquisition

MRI was performed using a 3 T MRI system (Discovery MR750w, GE Healthcare, Milwaukee, WI) using a 8-channel phased-array breast surface coil. Axial synthetic MR sequences and 2D MESE sequences for  $T_2$  mapping were added to the routine clinical MR sequences. The imaging parameters of additional sequences are summarized in Table 1.

Synthetic MRI data were acquired using MAGiC (MAGnetic resonance image Compilation) multi contrast MRI technique. The MAGiC sequence is a 2D spin echo multidynamic, multiecho sequence, which is performed using an interleaved slice-selective 120 degrees saturation and multiecho acquisition. This sequence includes two echo times and four automatically calculated saturation delays. With different combinations of echo time and saturation delay, each acquisition produced eight real images and eight imaginary images per section for the quantification of tissue physical properties, like longitudinal  $T_1$ , transverse  $T_2$  relaxation times and PD.

$T_2$  quantification was performed by using axial MESE sequence, with 16 echo times (TEs) from 9 to 147 ms. The  $T_2$  map from MESE was obtained using dedicated software (Discovery 750w, T2 Map; GE Healthcare). SyMRI software could automatically calculate the  $T_2$  values and make a  $T_2$  map in the GE 3 T scanner console. Figure 1 shows examples of synthetic MR images and  $T_2$  map.

Conventional MRI protocols included axial  $T_2$  weighted iterative decomposition of water and fat with echo asymmetry and

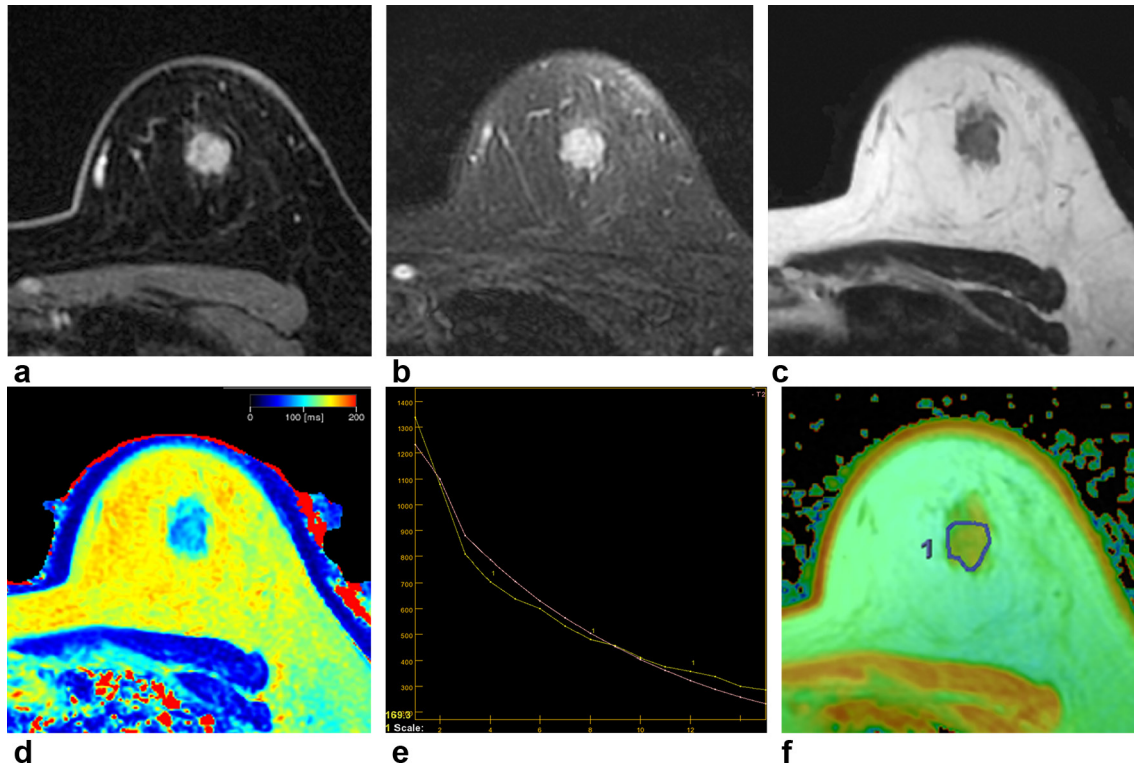
Table 1. MRI acquisition parameters

	Synthetic MRI	MESE $T_2$ mapping
TR (ms)	4000	1083
TE (ms)	2290	9,18,28,37,46,55,64,73,83,92,101,110,119,129,138,147
TI (ms)	130, 500, 1370, 2970 <sup>a</sup>	-
Flip angle	120	90
Field of view	34	30
Matrix	320 × 256	320 × 224
Section thickness (mm)	5	5
Interslice gap (mm)	5	5
Number of sections	26	14
Echo-train length	12	1
Acceleration factor	2	1
Acquisition time (min)	5 min 32 s	8 min 2 s

TE, echo time; TI, inversion time; TR, repetition time; MESE, multiecho spin echo;

<sup>a</sup>Four saturation delays, automatically calculated.

Figure 1. A 47-year-old female with invasive ductal carcinoma in the left breast. Contrast-enhanced axial image (a) shows an enhancing mass with irregular shape and margin in her left breast 12 o'clock direction.  $T_2$  weighted IDEAL fast spin echo image (b) shows an irregular mass showing high signal intensity in the same location. On synthetic  $T_2$  weighted image (c) and synthetic  $T_2$  map image (d), the  $T_2$  relaxation time was 87 ms. On MESE  $T_2$  mapping,  $T_2$  relaxation time can be measured using 16 different TEs (e). The x-axis indicates TEs and y-axis indicates the signal intensity (e). On MESE  $T_2$  mapping (f), the  $T_2$  relaxation time was 77.9 ms showing difference of 9.1 ms compared to synthetic  $T_2$  mapping. IDEAL, iterative decomposition of water and fat with echo asymmetry and least squares estimation; MESE, multi echo spin echo; TE, echo time.



least squares estimation fast spin echo image, axial short-time inversion recovery combination diffusion-weighted image and axial three-dimensional dynamic contrast enhanced  $T_2$  weighted images.

#### Image analysis

Synthetic  $T_2$ - and  $T_2$  weighted images were generated from multidynamic, multiecho data using a MAGiC, which is a customized version of synthetic MR's SyMRI software. Using both  $T_1$  and  $T_2$  maps, one radiologist with 9 years of experience in breast imaging drew region of interests (ROIs) manually along the tumor margins on two consecutive axial sections including the center of tumor mass. In each ROI,  $T_2$  relaxation time was automatically calculated and we used the mean value of two ROIs. For the measurement of  $T_2$  value of fat tissue, the radiologist drew an ROI in the subcutaneous fat of contralateral breast.

The longitudinal  $T_2$  relaxation time from MESE data was calculated using Functool software on Advantage Workstation (v. 4.5; General Electric Healthcare, Milwaukee, WI). The same radiologist drew ROIs manually with same manner and  $T_2$  relaxation time was automatically obtained.

#### Data analysis

Patients' medical records were reviewed to collect clinical and pathological data. Hormone receptor positivity was defined as estrogen receptor and/or progesterone receptor positivity ( $\geq 10\%$  nuclear staining) according to immunohistochemistry (IHC). Human epidermal growth factor receptor-2 (HER2) positivity was defined as an IHC HER2 score of 3+ or gene amplification by fluorescence *in situ* hybridization in tumors with an IHC HER2 score of 2+.

Black nuclear grade (nuclear Grade 1, poorly differentiated; Grade 2, moderately differentiated; and Grade 3, well differentiated) and modified Bloom-Richardson histological grade (histological Grade 1, well differentiated; Grade 2, moderately differentiated; and Grade 3, poorly differentiated) were also reviewed. For dichotomous-dependent variables, nuclear grade was classified as high (Grade 1) vs low (Grades 2 and 3) and histological grade as low (Grades 1 and 2) vs high (Grade 3).

Ki-67 expression was estimated as the percentage of tumor cells positively stained by the antibody. Ki-67 <14% was considered low and negative and Ki-67  $\geq 14\%$  was considered high and positive.

Table 2. Comparison of  $T_2$  relaxation time acquired by synthetic MRI and MESE  $T_2$  mapping in the breast cancer and fat tissue

	$T_2$ relaxation time acquired with synthetic MRI (ms)	$T_2$ relaxation time acquired with MESE $T_2$ mapping (ms)	Difference between synthetic MRI and MESE $T_2$ mapping (ms)
Cancer ( $n = 51$ )			
Mean $\pm$ SD	84.75 $\pm$ 15.54	90.35 $\pm$ 19.22	8.41 $\pm$ 5.8
Min ~ Max	56 ~ 134	46.4 ~ 136.1	0.2 ~ 23.2
Fat ( $n = 51$ )			
Mean $\pm$ SD	129.22 $\pm$ 9.53	102.11 $\pm$ 13.9	27.84 $\pm$ 12.96
Min ~ Max	107 ~ 146	70.2 ~ 142.5	4 ~ 54.1

MESE, multiecho spin echo; SD, standard deviation;

### Statistical analysis

To evaluate the difference of  $T_2$  values between synthetic MRI and MESE  $T_2$  mapping, we generated Bland–Altman plots. Spearman's correlation test was performed for the evaluation of correlations between  $T_2$  values obtained with synthetic MRI and MESE  $T_2$  mapping. Patients with lower differences than mean difference value were classified as little difference group and patients with higher differences than mean difference value were as large difference group.  $\chi^2$  test was used for the evaluation of relationships between the histopathologic factors and these two groups.

We used the SPSS 19.0 statistical software package (IBM, Armonk), with a value of  $p < 0.05$  considered to be significant.

### RESULTS

The mean  $T_2$  relaxation time of the cancer was 84.75 ms ( $\pm 15.54$ ) by synthetic MRI and 90.35 ms ( $\pm 19.22$ ) by MESE  $T_2$  mapping (Table 2). The mean  $T_2$  relaxation time of the fat was 129.22 ( $\pm 9.53$ ) and 102.11 ms ( $\pm 13.9$ ), respectively. Bland–Altman analysis showed mean difference of 8.4 ms and 95% limits of agreement ( $-3.0$  and 19.8 ms) for the breast cancer and a larger mean difference of 27.8 ms and 95% limits of agreement (2.4 and 53.2 ms) for the fat tissue of breast (Figure 2).

Spearman's correlation test showed that there was significant positive correlation between synthetic MRI and MESE sequences for the cancer ( $r = 0.713$ ,  $p < 0.001$ ) and for the fat ( $r = 0.551$ ,  $p < 0.001$ ).

We analyzed which histopathological factors were associated with the differences in  $T_2$  relaxation time of the cancer between synthetic MRI and MESE  $T_2$  mapping. The status of estrogen receptor was significantly correlated with the degree of differences ( $p = 0.02$ ) and the presence of estrogen receptor was more frequently observed in the group with little difference than the group with large difference. The histologic grade was also associated with the degree of differences ( $p = 0.043$ ) and the low histologic grade was more frequently observed in the group with little difference. Other histologic factors including nuclear grade, the progesterone receptor, HER2 and Ki-67 were not associated with the degree of difference (Table 3). Representative case is shown in Figure 1.

### DISCUSSION

Synthetic MRI is a promising acceleration MRI technique and radiologists can review multi-contrast images including  $T_1$ -,  $T_2$ -, PD-weighted images and inversion recovery images with one acquisition. Recently, the feasibility of synthetic MRI has been reported in the neuroimaging and musculoskeletal imaging.<sup>13–15,22–24</sup> In the study of Lee et al<sup>14</sup> the quality of  $T_1$ - and  $T_2$  weighted images were within the diagnostically acceptable range. The lesion conspicuity and differentiation of gray/white matter was comparable or better in synthetic  $T_1$ - and  $T_2$  weighted images. In the study of Yi et al<sup>24</sup> the diagnostic accuracy of synthetic MRI was similar to the conventional MRI for the diagnosis of cartilage lesions and tears of the cruciate ligament or meniscus.

Figure 2. Bland–Altman plots of  $T_2$  relaxation times of breast cancer (a) and fat (b). The y- and x-axes indicate the difference and average between synthetic MR and MESE sequences, respectively. The blue lines show the means of differences, while the 95% confidence intervals are denoted by the pairs of dotted red lines. MESE, multi echo spin echo.

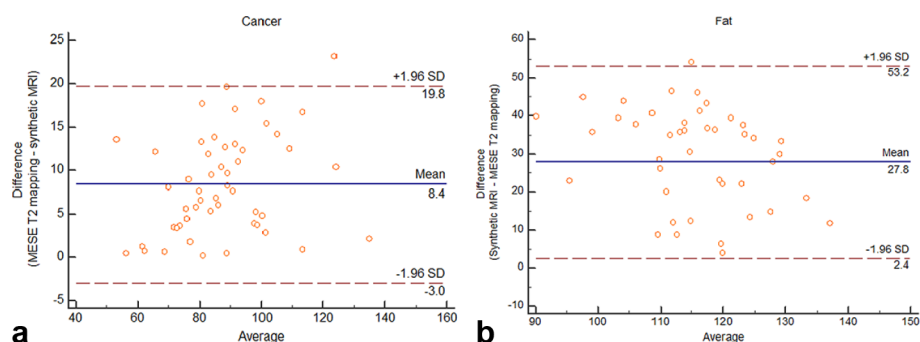


Table 3. Histopathologic factors associated with the differences between synthetic MRI and MESE  $T_2$  mapping

	Little difference between synthetic MRI and MESE $T_2$ mapping ( $n = 28$ )	Large difference between synthetic MRI and MESE $T_2$ mapping ( $n = 23$ )	$p$ -value
Histologic grade			0.043 <sup>a</sup>
Low ( $n = 38$ )	24 (85.7%)	14 (60.9%)	
High ( $n = 13$ )	4 (14.3%)	9 (39.1%)	
Nuclear grade			0.288
Low ( $n = 37$ )	22 (78.6%)	15 (65.2%)	
High ( $n = 14$ )	6 (21.4%)	8 (34.8%)	
Estrogen receptor			0.02 <sup>a</sup>
Positive ( $n = 37$ )	24 (85.7%)	13 (56.5%)	
Negative ( $n = 14$ )	4 (14.3%)	10 (43.5%)	
Progesterone receptor			0.603
Positive ( $n = 33$ )	19 (67.9%)	14 (60.9%)	
Negative ( $n = 18$ )	9 (32.1%)	9 (39.1%)	
HER2			0.577
Positive ( $n = 13$ )	8 (28.6%)	5 (21.7%)	
Negative ( $n = 38$ )	20 (71.4%)	18 (78.3%)	
Ki-67 <sup>b</sup>			0.292
Low ( $n = 13$ )	10 (43.5%)	3 (23.1%)	
High ( $n = 23$ )	13 (56.5%)	10 (76.9%)	

MESE, multiecho spin echo;

<sup>a</sup>Statistically significant

<sup>b</sup>The result of Ki-67 index was available in 36 patients.

In the current study, we applied synthetic MRI to the breast imaging and as far as we know, this is the first report in the breast imaging. Our results revealed that mean  $T_2$  value of breast cancer was 84.75 ms by synthetic MRI and 90.35 ms by MESE  $T_2$  mapping. Previous studies also reported similar  $T_2$  values to ours and it ranged from 75 to 82.7 ms.<sup>16-18</sup>

There are several studies reporting the clinical implication of  $T_2$  and  $T_2^*$  values of the breast cancer. In the study of Liu et al, the mean  $T_2$  relaxation time of malignant breast lesion was lower than that of benign lesions, 82.7 vs 95.5 ms.<sup>16</sup> They speculated that large size of cancer cells with abundant cytoplasm, lymphocyte/plasma cell infiltrations and necrotic materials in the intercellular space might cause reduced extracellular space and reduced free water content. This could account for the shorter  $T_2$  relaxation time in malignant breast lesions. Several studies reported the  $T_2$  and  $T_2^*$  values of breast cancer. Previous studies revealed that the mean  $T_2$  relaxation time of breast cancer had significantly decreased after neoadjuvant chemotherapy and  $T_2$  value of responders was significantly shorter than that of non-responders.<sup>17,18</sup> In the study of Seo et al,<sup>21</sup> the  $T_2^*$  relaxation time of invasive breast cancer was significantly longer than that of ductal carcinoma *in situ*. Among invasive breast cancers,  $T_2^*$  relaxation time was significantly longer in the cancers with higher histologic grades and high signal intensity on  $T_2$  weighted imaging.

As shown in Table 3, the relatively larger discrepancy above the mean difference was frequently observed in breast cancers with negative estrogen receptor and high histologic grade. We speculate that negative estrogen receptor and high histologic grade are associated with more aggressive form and more aggressive cancer might have more heterogeneous texture in its internal components. Thus, heterogeneous tissue characteristics could cause larger discrepancies in  $T_2$  values between synthetic MRI and MESE  $T_2$  mapping. Further research should be performed which tissue characteristics are associated with different  $T_2$  values and discrepancies between two sequences.

In our results, the mean  $T_2$  relaxation time of the fat was 129.22 ms with synthetic MRI and 102.11 ms with MESE  $T_2$  mapping showing a large mean difference of 27.8 ms. Many studies have reported the  $T_2$  relaxation time of the fat at 3 T with various measurement methods. There is a big dispersion of the reported  $T_2$  relaxation times of the fat ranging from 41 to 371 ms.<sup>25-29</sup> In the study of Rakow-Penner et al,  $T_2$  relaxation time of the fat was 52.96 ms at 3 T with TEs of 20 and 100 ms.<sup>26</sup> However, in the study of Edden et al,<sup>25</sup>  $T_2$  value of the fat was 154 ms showing higher  $T_2$  value compared to a previous study. They proposed that one likely reason of the higher  $T_2$  relaxation time was the use of a 32-echo readout compared with the single spin echo with TEs of 20 and 100 ms. Our synthetic MRI used similar TR and TE with the study by Rakow-Penner et al,<sup>26</sup> but the  $T_2$  values of

our study were much higher. The mechanism of synthetic MRI is very different from the MESE  $T_2$  mapping method for the acquisition of  $T_2$  values. In synthetic MRI, it used two different TEs and four different TI and it could make eight different kinds of images with different combination of each TE and TI. Thus, using eight images, SyMRI software automatically calculate the  $T_2$  values by the Bloch equation. Therefore, we speculate that this different mechanism of  $T_2$  value acquisition could be the main cause of the different  $T_2$  values.

Several factors including noise, partial volume effect and B1 effects could cause systematic errors and compromise the accuracy of the  $T_2$  relaxation times.<sup>30</sup> Furthermore, the MAGiC sequences are highly optimized for the brain tissue and the TEs are chosen automatically (22 and 90 ms). Therefore, the signal intensity of the fat with very long  $T_2$  values could be measured as inaccurate values.

There are many limitations in our study. First, we measured the  $T_2$  relaxation time of the cancer in two consecutive axial planes showing the largest diameter not in the whole tumor. Therefore,

the  $T_2$  value in our study did not represent the value of whole tumor. Second, some patients were excluded for the analysis because the cancer size was small and was not visualized on synthetic  $T_1$ - and  $T_2$  weighted images. This could cause a selection bias. Third, the sample size was relatively small to draw a solid conclusion. A larger study is needed to validate these results. Fourth, we did not evaluate the clinical implication of  $T_2$  relaxation time of the cancer, because the purpose of this study was only to compare the  $T_2$  values of synthetic MRI and MESE sequences. Further study should be performed about the effect of  $T_2$  relaxation time on the patients' prognosis.

In conclusion,  $T_2$  relaxation times of the breast cancer acquired with synthetic MRI showed positive correlation with those of MESE  $T_2$  mapping with acceptable difference range. However, the difference of  $T_2$  relaxation times in the fat was large in several cases and the adjustment of acquisition parameters could decrease the difference between two methods. Synthetic MRI could be useful for the evaluation of tissue characteristics by simultaneous acquisition of several quantitative physical properties.

## REFERENCES

- Obdeijn IM, Tilanus-Linthorst MM, Spronk S, van Deurzen CH, de Monye C, Hunink MG, et al. Preoperative breast MRI can reduce the rate of tumor-positive resection margins and reoperations in patients undergoing breast-conserving surgery. *AJR Am J Roentgenol* 2013; **200**: 304–10. doi: <https://doi.org/10.2214/AJR.12.9185>
- Hollingsworth AB, Stough RG, O'Dell CA, Brekke CE. Breast magnetic resonance imaging for preoperative locoregional staging. *Am J Surg* 2008; **196**: 389–97. doi: <https://doi.org/10.1016/j.amjsurg.2007.10.009>
- Debald M, Abramian A, Nemes L, Döbler M, Kaiser C, Keyver-Paik MD, et al. Who may benefit from preoperative breast MRI? A single-center analysis of 1102 consecutive patients with primary breast cancer. *Breast Cancer Res Treat* 2015; **153**: 531–7. doi: <https://doi.org/10.1007/s10549-015-3556-3>
- Berg WA, Zhang Z, Lehrer D, Jong RA, Pisano ED, Barr RG, et al. Detection of breast cancer with addition of annual screening ultrasound or a single screening MRI to mammography in women with elevated breast cancer risk. *JAMA* 2012; **307**: 1394–404. doi: <https://doi.org/10.1001/jama.2012.388>
- Passaperuma K, Warner E, Causer PA, Hill KA, Messner S, Wong JW, et al. Long-term results of screening with magnetic resonance imaging in women with BRCA mutations. *Br J Cancer* 2012; **107**: 24–30. doi: <https://doi.org/10.1038/bjc.2012.204>
- Warner E, Hill K, Causer P, Plewes D, Jong R, Yaffe M, et al. Prospective study of breast cancer incidence in women with a BRCA1 or BRCA2 mutation under surveillance with and without magnetic resonance imaging. *J Clin Oncol* 2011; **29**: 1664–9. doi: <https://doi.org/10.1200/JCO.2009.27.0835>
- Schacht DV, Yamaguchi K, Lai J, Kulkarni K, Sennett CA, Abe H. Importance of a personal history of breast cancer as a risk factor for the development of subsequent breast cancer: results from screening breast MRI. *AJR Am J Roentgenol* 2014; **202**: 289–92. doi: <https://doi.org/10.2214/AJR.13.11553>
- Belli P, Costantini M, Romani M, Marano P, Pastore G. Magnetic resonance imaging in breast cancer recurrence. *Breast Cancer Res Treat* 2002; **73**: 223–35. doi: <https://doi.org/10.1023/A:1015868406986>
- Cho N, Han W, Han BK, Bae MS, Ko ES, Nam SJ, et al. Breast Cancer Screening With Mammography Plus Ultrasonography or Magnetic Resonance Imaging in Women 50 Years or Younger at Diagnosis and Treated With Breast Conservation Therapy. *JAMA Oncol* 2017; **3**: 1495–502. doi: <https://doi.org/10.1001/jamaoncol.2017.1256>
- Kuhl CK, Schrading S, Strobel K, Schild HH, Hilgers RD, Bieling HB. Abbreviated breast magnetic resonance imaging (MRI): first postcontrast subtracted images and maximum-intensity projection—a novel approach to breast cancer screening with MRI. *J Clin Oncol* 2014; **32**: 2304–10. doi: <https://doi.org/10.1200/JCO.2013.52.5386>
- Warntjes JB, Leinhard OD, West J, Lundberg P. Rapid magnetic resonance quantification on the brain: Optimization for clinical usage. *Magn Reson Med* 2008; **60**: 320–9. doi: <https://doi.org/10.1002/mrm.21635>
- Warntjes JB, Dahlqvist O, Lundberg P. Novel method for rapid, simultaneous T1, T2\*, and proton density quantification. *Magn Reson Med* 2007; **57**: 528–37. doi: <https://doi.org/10.1002/mrm.21165>
- Granberg T, Uppman M, Hashim F, Cananau C, Nordin LE, Shams S, et al. Clinical Feasibility of Synthetic MRI in Multiple Sclerosis: A Diagnostic and Volumetric Validation Study. *AJNR Am J Neuroradiol* 2016; **37**: 1023–9. doi: <https://doi.org/10.3174/ajnr.A4665>
- Lee SM, Choi YH, Cheon JE, Kim IO, Cho SH, Kim WH, et al. Image quality at synthetic brain magnetic resonance imaging in children. *Pediatr Radiol* 2017; **47**: 1638–47. doi: <https://doi.org/10.1007/s00247-017-3913-y>
- Krauss W, Gunnarsson M, Andersson T, Thunberg P. Accuracy and reproducibility of a quantitative magnetic resonance imaging method for concurrent measurements of tissue relaxation times and proton density. *Magn Reson Imaging* 2015;

- 33: 584–91. doi: <https://doi.org/10.1016/j.mri.2015.02.013>
16. Liu L, Yin B, Shek K, Geng D, Lu Y, Wen J, et al. Role of quantitative analysis of T2 relaxation time in differentiating benign from malignant breast lesions. *J Int Med Res* 2018; **46**: 1928–35. doi: <https://doi.org/10.1177/0300060517721071>
  17. Liu L, Yin B, Geng DY, Lu YP, Peng WJ. Changes of T2 relaxation time from neoadjuvant chemotherapy in breast cancer lesions. *Iran J Radiol* 2016; **13**: e24014. doi: <https://doi.org/10.5812/iranradiol.24014>
  18. Tan PC, Pickles MD, Lowry M, Manton DJ, Turnbull LW, Lesion T. Lesion T(2) relaxation times and volumes predict the response of malignant breast lesions to neoadjuvant chemotherapy. *Magn Reson Imaging* 2008; **26**: 26–34. doi: <https://doi.org/10.1016/j.mri.2007.04.002>
  19. Uematsu T, Kasami M, Yuen S. Triple-negative breast cancer: correlation between MR imaging and pathologic findings. *Radiology* 2009; **250**: 638–47. doi: <https://doi.org/10.1148/radiol.2503081054>
  20. Bae MS, Shin SU, Ryu HS, Han W, Im SA, Park IA, et al. Pretreatment MR imaging features of triple-negative breast cancer: association with response to neoadjuvant chemotherapy and recurrence-free survival. *Radiology* 2016; **281**: 392–400. doi: <https://doi.org/10.1148/radiol.2016152331>
  21. Seo M, Ryu JK, Jahng GH, Sohn YM, Rhee SJ, Oh JH, et al. Estimation of T2\* relaxation time of breast cancer: correlation with clinical, imaging and pathological features. *Korean J Radiol* 2017; **18**: 238–48. doi: <https://doi.org/10.3348/kjr.2017.18.1.238>
  22. Betts AM, Leach JL, Jones BV, Zhang B, Serai S. Brain imaging with synthetic MR in children: clinical quality assessment. *Neuroradiology* 2016; **58**: 1017–26. doi: <https://doi.org/10.1007/s00234-016-1723-9>
  23. Park S, Kwack KS, Lee YJ, Gho SM, Lee HY. Initial experience with synthetic MRI of the knee at 3T: comparison with conventional T<sub>1</sub> weighted imaging and T<sub>2</sub> mapping. *Br J Radiol* 2017; **90**: 20170350. doi: <https://doi.org/10.1259/bjr.20170350>
  24. Yi J, Lee YH, Song HT, Suh JS. Clinical feasibility of synthetic magnetic resonance imaging in the diagnosis of internal derangements of the knee. *Korean J Radiol* 2018; **19**: 311–9. doi: <https://doi.org/10.3348/kjr.2018.19.2.311>
  25. Edden RA, Smith SA, Barker PB. Longitudinal and multi-echo transverse relaxation times of normal breast tissue at 3 Tesla. *J Magn Reson Imaging* 2010; **32**: 982–7. doi: <https://doi.org/10.1002/jmri.22306>
  26. Rakow-Penner R, Daniel B, Yu H, Sawyer-Glover A, Glover GH. Relaxation times of breast tissue at 1.5T and 3T measured using IDEAL. *J Magn Reson Imaging* 2006; **23**: 87–91. doi: <https://doi.org/10.1002/jmri.20469>
  27. Gold GE, Suh B, Sawyer-Glover A, Beaulieu C. Musculoskeletal MRI at 3.0 T: initial clinical experience. *AJR Am J Roentgenol* 2004; **183**: 1479–86. doi: <https://doi.org/10.2214/ajr.183.5.1831479>
  28. Bojorquez JZ, Bricq S, Brunotte F, Walker PM, Lalande A. A novel alternative to classify tissues from T<sub>1</sub> and T<sub>2</sub> relaxation times for prostate MRI. *MAGMA* 2016; **29**: 777–88. doi: <https://doi.org/10.1007/s10334-016-0562-3>
  29. de Bazelaire CM, Duhamel GD, Rofsky NM, Alsop DC. MR imaging relaxation times of abdominal and pelvic tissues measured in vivo at 3.0 T: preliminary results. *Radiology* 2004; **230**: 652–9. doi: <https://doi.org/10.1148/radiol.2303021331>
  30. Bojorquez JZ, Bricq S, Acquitter C, Brunotte F, Walker PM, Lalande A. What are normal relaxation times of tissues at 3 T? *Magn Reson Imaging* 2017; **35**: 69–80. doi: <https://doi.org/10.1016/j.mri.2016.08.021>